Kondo effect in alkaline-earth-metal atomic gases with confinement-induced resonances

Ren Zhang,[1] Deping Zhang,[1] Yanting Cheng,[1] Wei Chen,[1] Peng Zhang,[2,3,*] and Hui Zhai[1,†]

[1]*Institute for Advanced Study, Tsinghua University, Beijing 100084, China*

[2]*Department of Physics, Renmin University of China, Beijing 100872, China*

[3]*Beijing Key Laboratory of Opto-electronic Functional Materials & Micro-nano Devices, Renmin University of China, Beijing 100872, China*

(Received 28 September 2015; published 1 April 2016)

Alkaline-earth-metal atoms have a long-lived electronic excited state, and when atoms in this excited state are localized in the Fermi sea of ground-state atoms by an external potential, they serve as magnetic impurities, due to the spin-exchange interaction between the excited- and the ground-state atoms. This can give rise to the Kondo effect. However, in order to achieve this effect in current atomic gas experiments, it requires the Kondo temperature to be increased to a sizable portion of the Fermi temperature. In this paper we calculate the confinement-induced resonance (CIR) for the spin-exchanging interaction between the ground and the excited states of the alkaline-earth-metal atoms and propose that the spin-exchange interaction can be strongly enhanced by utilizing the CIR. We analyze this system by the renormalization-group approach and show that near a CIR, the Kondo temperature can be significantly enhanced.

DOI: 10.1103/PhysRevA.93.043601

I. INTRODUCTION

Cold alkaline-earth-metal atomic gases have been widely used for building atomic clocks, with which the record of the most accurate optical lattice clock has been achieved [1]. This is because alkaline-earth-metal atoms have a very-long-lived excited $^3P_0$ state whose single-particle lifetime can be as long as many seconds. This excited $^3P_0$ state and the ground $^1S_0$ state are viewed as two internal states of the orbital degree of freedom. Recently, there has been increasing experimental interest in studying many-body physics with alkaline-earth-metal atoms, including the SU(N) symmetric interaction and the orbital degree of freedom [2–7]. In particular, recent experiments have demonstrated the interorbital spin-exchange scattering between the ground state $^1S_0$ and this $^3P_0$ state in fermionic ^{88}Sr [4] and ^{173}Yb atoms [5,6].

Utilizing different ac polarizability of $^1S_0$ and $^3P_0$ states, one can realize the situation that atoms in the $^3P_0$ state experience a deep lattice and are localized, while atoms in the $^1S_0$ states experience a shallow lattice and remain itinerant, as shown in Fig. 1. Therefore, due to the spin-exchange scattering between these two states, atoms in the $^3P_0$ state can play the role of magnetic impurities in the Fermi sea of atoms in the $^1S_0$ state, which can give rise to the Kondo effect [8]. Realizing the Kondo effect with cold atoms [8–17] can add a few new components of the Kondo physics, such as the SU(N) Kondo model and manifestation of the Kondo effect other than transport properties and nonequilibrium dynamics. When the magnetic coupling is much weaker compared to the Fermi energy, such as in the cases of solid-state materials, the Kondo temperature is a few orders of magnitude lower than the Fermi temperature. However, with the current cooling power, normally an atomic Fermi gas can only be cooled to $\sim 0.1T_F$ (T_F denotes the Fermi temperature). Therefore, the most challenging question is how to increase the Kondo temperature to the range attainable by current experiments.

In this paper we propose a scheme to overcome this challenge by using confinement-induced resonance (CIR). The CIR phenomenon describes resonant enhancement of the one-dimensional (1D) effective interaction strength when a system is confined in a quasi-one-dimensional tube [18,19]. This phenomenon has been observed in previous cold-atom experiments with alkali-metal atoms [20]. Here we generalize the CIR phenomenon to the interorbital scattering between $^1S_0$ and $^3P_0$ states of alkaline-earth-metal atoms. We will show that a CIR can strongly enhance the spin-exchange scattering and consequently the Kondo temperature can be increased to a sizable fractional of the Fermi temperature when a CIR is approached.

II. CONFINEMENT-INDUCED RESONANCE

A. Zero magnetic field

To illustrate the basic ideas, we first discuss a two-body problem at zero magnetic field. Let us briefly review the interaction between two fermions in two different orbital states $^3P_0$ (denoted by $|e\rangle$) and $^1S_0$ (denoted by $|g\rangle$) and different nuclear spin states (for simplicity, here we only take two nuclear spin states denoted by $|\uparrow\rangle$ and $|\downarrow\rangle$), respectively. We can introduce four antisymmetric bases for the internal degrees of freedom

$$|\pm\rangle = \frac{1}{2}(|ge\rangle \pm |eg\rangle)(|\uparrow\downarrow\rangle \mp |\downarrow\uparrow\rangle), \tag{1}$$

$$|g\uparrow; e\uparrow\rangle = \frac{1}{\sqrt{2}}(|ge\rangle - |eg\rangle)|\uparrow\uparrow\rangle, \tag{2}$$

$$|g\downarrow; e\downarrow\rangle = \frac{1}{\sqrt{2}}(|ge\rangle - |eg\rangle)|\downarrow\downarrow\rangle, \tag{3}$$

in which s-wave scattering is allowed. Here $|+\rangle$ is an orbital triplet and nuclear spin singlet and the other three are an orbital singlet and nuclear spin triplet. Since nuclear spin does not participate in the interatomic interaction process, the interaction part possesses the nuclear spin rotational symmetry, for which the spin singlet and triplet will not mix and the interaction potentials are the same for $|-\rangle$ and $|g\uparrow; e\uparrow\rangle$ and

*pengzhang@ruc.edu.cn

†hzhai@tsinghua.edu.cn

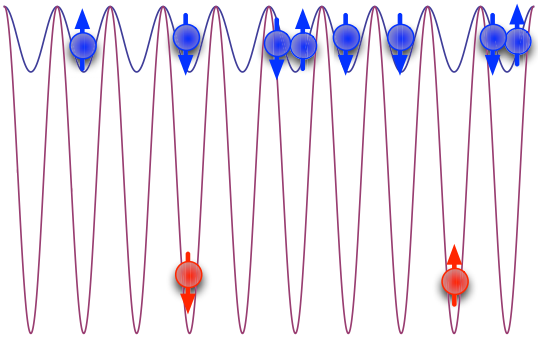

FIG. 1. Schematic of the system under consideration. The red balls are alkaline-earth-metal atoms in the $^3P_0$ state. They are trapped in a deep lattice, are localized, and have a lower density. The blue balls are alkaline-earth-metal atoms in the $^1S_0$ state. They are trapped in a shallow lattice and are itinerant. The arrows denote the nuclear spin degree of freedom. The system is confined in a one-dimensional tube.

$|g\downarrow;e\downarrow\rangle$ channels. Therefore, the interatomic potential $\hat{V}(\mathbf{r})$ is diagonal in the bases $\{|+\rangle,|-\rangle,|g\uparrow;e\uparrow\rangle,|g\downarrow;e\downarrow\rangle\}$ as

$$V_+(\mathbf{r})\mathcal{P}_+ + V_-(\mathbf{r})(\mathcal{P}_- + \mathcal{P}_{\uparrow\uparrow} + \mathcal{P}_{\downarrow\downarrow}),$$

where $\mathcal{P}_i = |i\rangle\langle i|$ $(i = \pm)$, $\mathcal{P}_{\uparrow\uparrow} = |g\uparrow;e\uparrow\rangle\langle g\uparrow;e\uparrow|$, and $\mathcal{P}_{\downarrow\downarrow} = |g\downarrow;e\downarrow\rangle\langle g\downarrow;e\downarrow|$. The two interaction potentials are denoted by $V_\pm(\mathbf{r}) = 2\pi\hbar^2 a_\pm \delta(\mathbf{r})\frac{\partial}{\partial r}(r)/\mu$ where μ is the two-body reduced mass and $a_\pm$ are two independent scattering lengths.

We can rotate the interaction potential $\hat{V}(\mathbf{r})$ in other bases $\{|g\uparrow;e\downarrow\rangle,|g\downarrow;e\uparrow\rangle,|g\uparrow;e\uparrow\rangle,|g\downarrow;e\downarrow\rangle\}$, where $|g\uparrow;e\downarrow\rangle = (1/\sqrt{2})(|+\rangle + |-\rangle)$ and $|g\downarrow;e\uparrow\rangle = (1/\sqrt{2})(|-\rangle - |+\rangle)$, and $V(\mathbf{r})$ becomes

$$\hat{V} = \frac{V_+ + V_-}{2}(\mathcal{P}_{\uparrow\downarrow} + \mathcal{P}_{\downarrow\uparrow}) + \frac{V_- - V_+}{2}(\mathcal{S}_{\rm ex} + \mathcal{S}_{\rm ex}^\dagger) + V_-(\mathcal{P}_{\uparrow\uparrow} + \mathcal{P}_{\downarrow\downarrow}), \tag{4}$$

where $\mathcal{P}_{\uparrow\downarrow} = |g\uparrow;e\downarrow\rangle\langle g\uparrow;e\downarrow|$, $\mathcal{P}_{\downarrow\uparrow} = |g\downarrow;e\uparrow\rangle\langle g\downarrow;e\uparrow|$, and $\mathcal{S}_{\rm ex} = |g\uparrow;e\downarrow\rangle\langle g\downarrow;e\uparrow|$. In the presence of a lattice as described in Fig. 1, when atoms in the $|e\rangle$ state are localized as impurities while atoms in the $|g\rangle$ state remain itinerant, the off-diagonal $(V_- - V_+)/2$ represents the process that an itinerant fermion exchanges its spins with impurities and this spin-exchange process is the essential process responsible for the Kondo effect [21]. Normally, this interaction strength is much smaller compared to the Fermi energy and the Kondo temperature is exponentially suppressed [21].

Now let us consider atoms confined in a quasi-one-dimensional tube by a transverse harmonic trap. Here we consider the situation that the transverse confinement is the same for both $^3P_0$ and $^1S_0$ states, which can be achieved by applying a two-dimensional optical lattice in the x-y plane with the magic wavelength [22]. We first consider the situation without a lattice along the longitudinal z direction. The free Hamiltonian $\hat{H}_0$ can be separated into the center-of-mass part and the relative motion part $\hat{H}_{\rm r}$, where

$$\hat{H}_{\rm r} = -\frac{\hbar^2}{2\mu}\nabla_{\mathbf{r}}^2 + \frac{\mu\omega^2}{2}(x^2 + y^2). \tag{5}$$

For a single interaction channel with a three-dimensional scattering length $a_{\rm s}$, it is known that the interaction strength of the effective one-dimensional interaction potential $g_0\delta(z)$ is given by [18]

$$g_0 = \frac{2\pi\hbar^2 a_{\rm s}}{\mu}|\phi_{00}|^2\left(1 - \mathcal{C}\frac{a_{\rm s}}{a_\perp}\right)^{-1}, \tag{6}$$

where ϕ_{00} is the ground-state wave function of $\hat{H}_{\rm r}$, $a_\perp = \sqrt{\mu\omega/\hbar}$ is the harmonic length, and $\mathcal{C} = 1.4603\ldots$ is a constant. Here g diverges when $a_\perp = \mathcal{C}a_{\rm s}$, which is known as CIR [18]. This resonance occurs when the energy of a bound state in the transverse excited modes matches the scattering threshold [19].

At zero field, it is easy to show that $|+\rangle$, $|-\rangle$, $|g\uparrow;e\uparrow\rangle$, and $|g\downarrow;e\downarrow\rangle$ are all eigenstates of the free Hamiltonian $\hat{H}_0$. Hence, under confinement, these four scattering channels can be treated as independent channels and the reduced one-dimensional interaction still takes a diagonal form as

$$\hat{V}_{\rm 1D} = [g_+\mathcal{P}_+ + g_-\mathcal{P}_- + g_0\mathcal{P}_{\uparrow\uparrow} + g_0\mathcal{P}_{\downarrow\downarrow}]\delta(z), \tag{7}$$

where g_+ is related to a_+ and g_-, g_0 are related to a_- via Eq. (6). Therefore, when rotated to the $\{|g\uparrow;e\downarrow\rangle,|g\downarrow;e\uparrow\rangle,|g\uparrow;e\uparrow\rangle,|g\downarrow;e\downarrow\rangle\}$ bases, the spin-exchange interaction term is now given by $(g_- - g_+)\delta(z)/2$. When $a_\perp \to \mathcal{C}a_+$, g_+ diverges and g_- remains finite and when $a_\perp \to \mathcal{C}a_-$, g_- diverges and g_+ remains finite, as shown in Fig. 2(a). Therefore, the spin-exchange interaction becomes very strong near these two CIRs and consequently the Kondo temperature can be dramatically enhanced. This is the basic idea of our proposal.

B. Finite magnetic field

In a real experiment there is always a finite magnetic field. Due to the difference in the Landé g-factor between $|g\rangle$ and $|e\rangle$ states, the $|g\uparrow;e\downarrow\rangle$ and $|g\downarrow;e\uparrow\rangle$ states differ by a finite energy δ proportional to the magnetic-field strength [25]. In other words, this leads to a mixing term between $|+\rangle$ and $|-\rangle$ given by $\delta/2(|+\rangle\langle -| + \text{H.c.})$ [5,6]. Therefore, these two channels can no longer be treated independently, which presents an additional complication for our proposal. Under the condition $\delta \ll \hbar\omega$, both channels are retained in the one-dimensional effective mode. To deduce the one-dimensional interactional strength, our calculation follows the standard procedure of CIR discussed before [18], that is, one first obtains an effective one-dimensional scattering amplitude in both the $|g\uparrow;e\downarrow\rangle$ and $|g\downarrow;e\uparrow\rangle$ channels by solving the three-dimensional Hamiltonian with the confinement potential and then constructs an effective one-dimensional model that gives exactly the same scattering amplitude.

The Hamiltonian for the relative motion of the two-body system with a confinement potential can be written as

$$\hat{H}_c = \left[-\frac{\hbar^2}{2\mu}\nabla_{\mathbf{r}}^2 + \frac{\mu\omega^2}{2}(x^2 + y^2)\right](\mathcal{P}_+ + \mathcal{P}_-) + \frac{\delta}{2}(\mathcal{S}_c + \mathcal{S}_c^\dagger) + V_+(\mathbf{r})\mathcal{P}_+ + V_-(\mathbf{r})(\mathcal{P}_- + \mathcal{P}_{\uparrow\uparrow} + \mathcal{P}_{\downarrow\downarrow}), \tag{8}$$

where $\mathcal{S}_c = |+\rangle\langle -|$. Two important features at finite δ are worth emphasizing here. First, in three dimensions, the

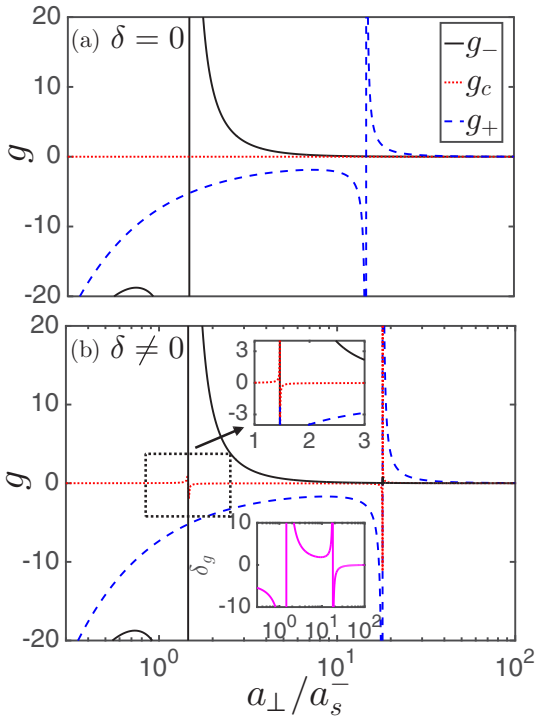

FIG. 2. One-dimensional interaction strengths g_+, g_-, and g_c ($\hbar^2/\mu 10^3 a_0$ is taken as the unit) as a function of $a_\perp/a_s^-$ for the magnetic field (a) $B = 0$, where $g_c = 0$, and (b) $B = 35$ G, where we use ^{173}Yb as an example and take $\delta = 2\pi \times (112\ \text{Hz/G})\hbar\text{B}$, and therefore $\delta = 25\ \text{kHz}\hbar$ at 35 G. In both cases, g_0 always behaves the same as g_- in case (a). For ^{173}Yb we take $a_+ \simeq 10a_-$ and $a_- = 200a_0$ [23,24]. The first CIR takes place around $a_\perp \approx \mathcal{C}a_-$ and the second CIR takes place around $a_\perp \approx \mathcal{C}a_+$, though the exact locations of the CIRs will be shifted by the magnetic field. The insets in (b) show g's near the first CIR and $\delta g = g_- - g_+$.

interaction does not mix $|+\rangle$ and $|-\rangle$ because it respects the nuclear spin rotational symmetry. However, the finite Zeeman field δ in the single-particle Hamiltonian breaks the nuclear spin rotational symmetry. In the quasi-one-dimensional system, since the virtual processes to the transverse excited levels are taken into account when reducing dimensionality, the effect of this Zeeman energy term enters the effective one-dimensional interaction term $\hat{V}_{1\text{D}}$ through the intermediate state energy of these virtual processes. Hence, the effective 1D Hamiltonian is expected to take the form

$$\hat{H}_{1\text{D}} = \left(-\frac{\hbar^2}{2\mu}\frac{d^2}{dz^2}\right)(\mathcal{P}_+ + \mathcal{P}_-) + \frac{\delta}{2}(\mathcal{S}_c + \mathcal{S}_c^\dagger) + V_{1\text{D}}, \quad (9)$$

where

$$\hat{V}_{1\text{D}} = [g_+\mathcal{P}_+ + g_-\mathcal{P}_- + g_c(\mathcal{S}_c + \mathcal{S}_c^\dagger) + g_0(\mathcal{P}_{\uparrow\uparrow} + \mathcal{P}_{\downarrow\downarrow})]\delta(z). \quad (10)$$

It should be noted that $V_{1\text{D}}$ no longer respects the nuclear spin rotational symmetry and contains a nonzero off-diagonal term g_c that couples the $|+\rangle$ and $|-\rangle$ channels. A similar effect has also been discussed in the CIR of spinor atoms [26]. Here g_+, g_-, and g_c depend on the strength of the Zeeman field, as shown in Fig. 2(b). The detailed derivation of these parameters are given in the Appendix, while the g_0 are still related to a_- via Eq. (6) since the $|g\uparrow; e\uparrow\rangle$ and $|g\downarrow; e\downarrow\rangle$ states are still eigenstates despite the presence of the Zeeman term.

Second, when g_+ diverges, g_- and g_c will also diverge, as shown in Fig. 2(b), and similarly when g_- diverges. After the base rotation, the interaction term becomes

$$\hat{H}_{\text{int}} = \left[\left(\frac{g_+ + g_-}{2} + g_c\right)\mathcal{P}_{\uparrow\downarrow} + \left(\frac{g_+ + g_-}{2} - g_c\right)\mathcal{P}_{\downarrow\uparrow} + \frac{g_- - g_+}{2}(\mathcal{S}_{\text{ex}} + \mathcal{S}_{\text{ex}}^\dagger) + g_0(\mathcal{P}_{\uparrow\uparrow} + \mathcal{P}_{\downarrow\downarrow})\right]\delta(z), \quad (11)$$

where the spin-exchange term is still given by $(g_- - g_+)\delta(z)/2$. Fortunately, as shown in Fig. 2(b), one can see that near one of the CIRs, either g_- diverges much slower than g_+ or g_+ diverges much slower than g_-. Therefore, $(g_- - g_+)/2$ still displays a divergent behavior and the insight gained from the zero-field limit will hold.

III. KONDO EFFECT

A. Lattice model with a single impurity

Now we consider turning on the lattice potential as shown in Fig. 1, which localizes atoms in the $|e\rangle$ state as impurities in a Fermi sea of atoms in the $|g\rangle$ state. We also consider the regime where the density of impurity atoms is much more dilute than the density of itinerant atoms and for simplicity we consider a single impurity problem. The tight-binding model is given by

$$\hat{H} = \hat{H}_0 + \hat{H}_{\text{I}}, \quad (12)$$

$$\hat{H}_0 = \sum_{k,\sigma}(-t\cos k)c_{k\sigma}^\dagger c_{k\sigma} + \delta S^z/2 - \frac{\delta}{2L}\sum_k s_{kk}^z, \quad (13)$$

$$\hat{H}_{\text{I}} = \frac{1}{L}\sum_{k,q}\left\{\frac{J_+}{2}S^+ s_{kq}^- + \frac{J_-}{2}S^- s_{kq}^+ + \frac{J_z}{2}S^z s_{kq}^z + U n_{kq} + \frac{U_1}{2}S^z n_{kq} + U_2 s_{kq}^z\right\}, \quad (14)$$

where $c_{k\sigma}$ and d_σ are fermion operators for itinerant fermions and impurity fermion, respectively, $S^+ = d_\uparrow^\dagger d_\downarrow$, $S^- = d_\downarrow^\dagger d_\uparrow$, $S^z = (1/2)(d_\uparrow^\dagger d_\uparrow - d_\downarrow^\dagger d_\downarrow)$, $s_{kq}^- = c_{k,\downarrow}^\dagger c_{q,\uparrow}$, $s_{kq}^+ = c_{k,\uparrow}^\dagger c_{q,\downarrow}$, $s_{kq}^z = (1/2)(c_{k,\uparrow}^\dagger c_{q,\uparrow} - c_{k,\downarrow}^\dagger c_{q,\downarrow})$, and $n_{kq} = c_{k,\uparrow}^\dagger c_{q,\uparrow} + c_{k,\downarrow}^\dagger c_{q,\downarrow}$. In addition, t is the hopping amplitude of itinerant fermions. The interaction parameters $J_\perp$, J_z, U_z, U_+, and U_- are related to g_+, g_-, and g_c via

$$J_\pm \propto -(g_+ - g_-), \quad J_z \propto -(g_+ + g_- - 2g_0), \quad (15)$$

$$U \propto \frac{g_+ + g_- + 2g_0}{4}, \quad U_1 \propto -2g_c, \quad U_2 \propto g_c, \quad (16)$$

where the proportional constant depends on the details of the Wannier function overlap between localized atoms and itinerant atoms (in the following figures, this constant has been chosen as 0.03).

Here we discuss a few features of this lattice model.

(i) The first three terms ($J_\pm$ and J_z terms) in $\hat{H}_{\text{I}}$ describe the Kondo coupling. From Fig. 2 one can see that (a) on the

left side of the first CIR and the right side of the second CIR, $J_\pm, J_z < 0$ and (b) on the right side of the first CIR and the left side of the second CIR, $J_\pm, J_z > 0$. Thus, both ferromagnetic and antiferromagnetic Kondo couplings can be accessed by tuning the confinement length $a_\perp$. At zero field, when $g_0 = g_-$, from Eq. (15) we have $J_\pm = J_z$ and the Kondo coupling respects spin-rotational symmetry, while at finite Zeeman field, generally g_0 is not equal to g_- and it gives rise to an anisotropic Kondo model.

(ii) The fourth term (U term) in $\hat{H}_{\rm I}$ describes a potential scattering that does not depend on spins. This comes from the diagonal term in Eq. (11). Furthermore, at finite field, due to the absence of the full spin rotational symmetry (a rotational symmetry along the spin z axis is still present), there exist two other scattering terms (U_1 and U_2 terms) in $\hat{H}_{\rm I}$. It naturally raises the question of whether these extra terms will affect the Kondo physics.

(iii) The δ term in $\hat{H}_0$ comes from the different g-factor between localized and itinerant fermions. When this term is sufficiently large, it tends to polarize fermions and will destroy the Kondo physics.

We remark that here the interaction between itinerant fermions is ignored since microscopically it is described by another independent scattering length between atoms in $|g\rangle$ states with different nuclear spins (normally denoted by $a_{\rm gg}$.) The CIR for $a_{\rm gg}$ is reached at a different confinement radius when $a_\perp = \mathcal{C}a_{\rm gg}$, where the interaction between itinerant fermions will become very strong. With interactions, the effect of a magnetic impurity in a Luttinger liquid has been studied before [27,28], and in the strongly interaction limit the results will be reported elsewhere [29]. In contrast, at the two CIRs we focus on here, this interaction is rather weak and can be safely ignored.

B. Renormalization-group studies

To address the effect of these extra terms and to make a more concrete predication of the Kondo temperature, here we adopt the renormalization-group (RG) approach well established for the Kondo problem [21,30]. The key idea is to iteratively integrate out the high-energy modes of itinerant fermions and see how the interaction parameters flow. In this analysis we only consider the lowest-order virtual processes. For simplicity, only the scattering processes that renormalize J_- are shown explicitly in Fig. 3 as an example. The renormalization to the J_- term from the processes in Fig. 3(a) when the cutoff is reduced from D to $D - \delta D$ reads

$$\begin{aligned}&\sum_p \frac{J_-}{2} S^- c^\dagger_{k,\uparrow} c_{p,\downarrow} \frac{1}{\omega + \epsilon_q - \epsilon_p} \frac{J_{z\downarrow}}{2} S^z c^\dagger_{p,\downarrow} c_{q,\downarrow} \\ &\approx \frac{J_{z\downarrow} J_-}{4} S^- S^z \rho_0 |\delta D| c^\dagger_{k\uparrow} c_{q\downarrow} \frac{1}{-D} \\ &= -\frac{1}{8} J_{z\downarrow} J_- \rho_0 |\delta D| S^- c^\dagger_{k\uparrow} c_{q\downarrow} \frac{1}{D}, \end{aligned} \tag{17}$$

where ρ_0 is the density of states of the itinerant atoms near the Fermi surface and we have set $c_p c^\dagger_p = 1$ for the p states in the energy scale between D and $D - \delta D$ and $S^z = 1/2$ for up-spin impurity. The approximation in Eq. (17) comes from the fact that $\epsilon_p \approx D$ and $D \gg \omega, \epsilon_q$. Similarly, one can

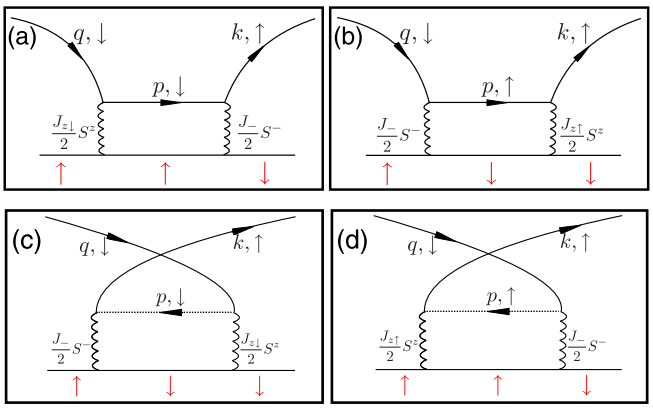

FIG. 3. Second-order diagram that can renormalize J_- for (a) and (b) the particle process and (c) and (d) the hole process. Black arrows denote the itinerant atomic spin and red arrows denote the impurity atomic spin.

write the renormalization contribution to the J_- term from Figs. 3(b)–3(d) as

$$\frac{1}{8} J_{z\uparrow} J_- \rho_0 |\delta D| S^- c^\dagger_{k\uparrow} c_{q\downarrow} \frac{1}{D+\delta}, \tag{18}$$

$$-\frac{1}{8} J_{z\downarrow} J_- \rho_0 |\delta D| S^- c^\dagger_{k\uparrow} c_{q\downarrow} \frac{1}{D+\delta}, \tag{19}$$

$$\frac{1}{8} J_{z\uparrow} J_- \rho_0 |\delta D| S^- c^\dagger_{k\uparrow} c_{q\downarrow} \frac{1}{D}. \tag{20}$$

It turns out that the contribution of the diagrams that involve the U_σ term is zero. Thus one can sum up all the diagrams and obtain the renormalization equation for J_- as

$$\frac{dJ_-}{dD} = \frac{\rho_0}{4} J_-(J_{z\downarrow} - J_{z\uparrow}) \left(\frac{1}{D+\delta} + \frac{1}{D} \right). \tag{21}$$

By repeating similar procedures, one can find the renormalization equations of all the interaction parameters in Eq. (14) as follows:

$$\frac{dJ_+}{dD} = -\frac{\rho_0}{2} J_+ J_z \left(\frac{1}{D-\delta} + \frac{1}{D} \right), \tag{22}$$

$$\frac{dJ_-}{dD} = -\frac{\rho_0}{2} J_- J_z \left(\frac{1}{D+\delta} + \frac{1}{D} \right), \tag{23}$$

$$\frac{dJ_z}{dD} = -\frac{\rho_0}{2} J_+ J_- \left(\frac{1}{D-\delta} + \frac{1}{D+\delta} \right), \tag{24}$$

$$\frac{dU_2}{dD} = \frac{\rho_0}{4} J_+ J_- \left(\frac{1}{D-\delta} - \frac{1}{D+\delta} \right), \tag{25}$$

$$\frac{dU_1}{dD} = 0, \quad \frac{dU}{dD} = 0, \tag{26}$$

where we have taken D as the energy cutoff and its initial value is chosen to be an energy scale of the order of the Fermi energy. For simplicity, we have also assumed a constant density of state denoted by ρ_0. When $\delta = 0$, Eq. (26) can be reduced to the RG equations derived in Ref. [30]. At this level of approximation, the U and U_1 terms are renormalized.

Here we focus on the antiferromagnetic case. In Fig. 4(a) we show a typical flow of the RG equations with $\delta \ll E_{\rm F}$. We find that upon lowering the energy cutoff, the $J_\pm$ and J_z terms

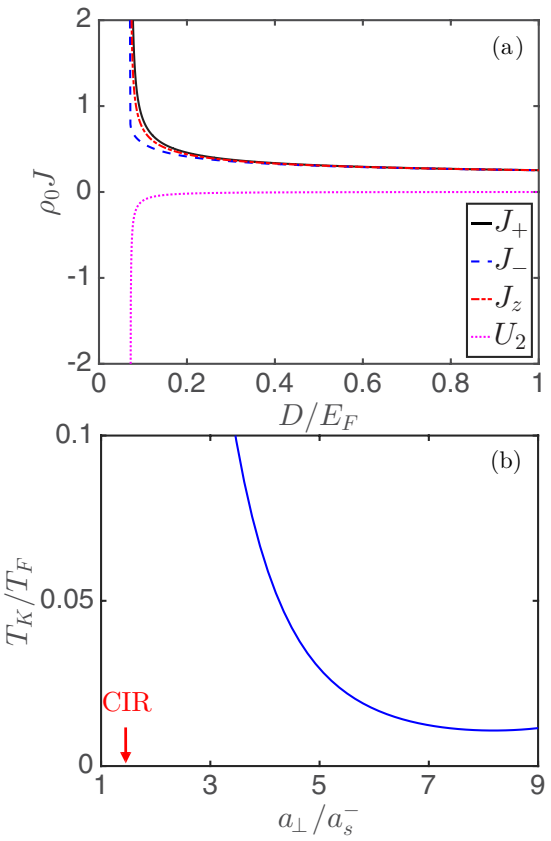

FIG. 4. (a) Flow of parameters $J_\pm$, J_z, and U_2 for lowering energy cutoff D. Here we have taken a typical density that gives rise to $E_F = 5\hbar \times 10^4$ Hz and the initial values of $J_\pm$, J_z, and U_2 as $\rho_0 J_\pm = 0.2377$, $\rho_0 J_z = 0.2376$, and $\rho_0 U_z = -3 \times 10^{-4}$. (b) The Kondo temperature increases as the confinement length $a_\perp$ is tuned toward the first CIR from the antiferromagnetic coupling side. Here we have taken $\delta = 0.07 E_F$.

diverge much faster than the U_2 term. This in fact can already be seen in the RG equation, since dU_2/dD scales with δ/D^2 and therefore evolves very slowly when $\delta \ll D$. Thus, at the energy scale when $J_\pm$ and J_z diverge, the Kondo effect appears while the strength of other terms remains quite small. Hence, we conclude that the extra interaction terms in the lattice model (14) will not affect the Kondo effect in this system.

The divergent energy scale for $J_\pm$ and J_z is normally taken as the Kondo temperature [21]. In Fig. 4(b) we show the dramatic increase of the Kondo temperature upon approaching one of the CIRs. The Kondo temperature can increase to $\sim 0.1 T_F$, which is attainable by current experiments. The underlying physics is basically the increasing of spin-exchange coupling as we discussed above. In the plot of Fig. 4(b) we have restricted out initial interaction parameter $\rho_0 J_\pm, \rho_0 J_z \lesssim 0.2$. When it is very close to the CIR, the initial value of these interaction parameters are already very large, which invalidates the perturbative RG approach. The impurity physics with a large or even divergent spin-exchange interaction remains a challenging issue and this makes the experimental quantum simulation studies of this model even more interesting.

Solving the RG equations for $\delta \sim E_F$ or $\delta \gg E_F$, we find none of the interaction parameters will diverge even when the cutoff D is lowered to zero as shown in Fig. 5, which means the absence of the Kondo effect. Therefore, for a fixed $a_\perp/a_s$, increasing δ simply by increasing the magnetic field can drive a crossover from a Kondo regime to a non-Kondo regime.

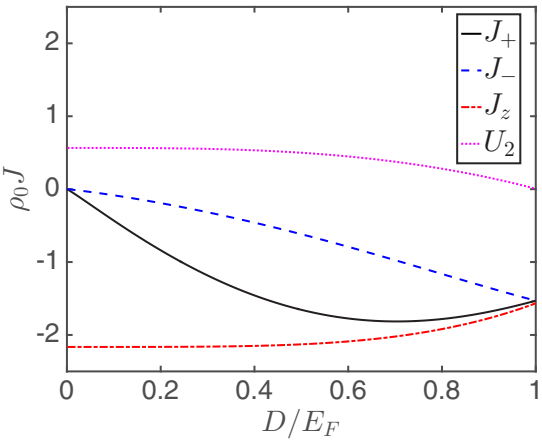

FIG. 5. The RG flow of parameters $J_\pm$, J_z, and U_2 in a strong magnetic field with $B = 100$ G and $\delta/E_F \simeq 1.4$.

IV. CONCLUSION

We have studied the CIR for two-orbital alkaline-earth-metal atoms with interorbital spin-exchange interaction at finite magnetic field. We show that the CIR can strongly enhance the spin-exchange scattering and hence dramatically increase the Kondo temperature. The signature of the Kondo effect will manifest not only in the transport properties, but also in other quantities such as spin susceptibility that can be measured by a cold-atom experiment [31]. Our proposal is very useful to ongoing experiments on many-body physics with alkaline-earth-metal atoms.

ACKNOWLEDGMENTS

This work was supported by Tsinghua University Initiative Scientific Research Program; NSFC Grants No. 11174176 (H.Z.), No. 11325418 (H.Z.), No. 11222430 (P.Z.), No. 11434011 (P.Z.), and No. 11504195 (W.C.); and NKBRSFC under Grants No. 2011CB921500 (H.Z.) and No. 2012CB922104 (P.Z.).

APPENDIX: CONFINEMENT-INDUCED RESONANCE AT FINITE MAGNETIC FIELD

To determine g_+, g_-, and g_c, we can rewrite the Hamiltonian in Eq. (8) as

$$\hat{H}_c = \left[-\frac{\hbar^2}{2\mu}\nabla_{\mathbf{r}}^2 + \frac{\mu\omega^2}{2}(x^2+y^2) + V_0\right](\mathcal{P}_{\uparrow\downarrow} + \mathcal{P}_{\downarrow\uparrow}) + \delta\mathcal{P}_{\uparrow\downarrow} + V_1(\mathcal{S}_{\rm ex} + \mathcal{S}_{\rm ex}^\dagger), \tag{A1}$$

where it is not necessary to consider the $|g\uparrow; e\uparrow\rangle$ and $|g\downarrow; e\downarrow\rangle$ channels at present since they do not couple to other channels even in the presence of a magnetic field. Here the operators V_0 and V_1 are given by $V_i = 2\pi\hbar^2 a_{si}\delta(\mathbf{r})\frac{\partial}{\partial r}(r)/\mu$ $(i = 1,2)$ with $a_{s0} = (a_s^+ + a_s^-)/2$ and $a_{s1} = (a_s^- - a_s^+)/2$. In Eq. (A1)

we have shifted the threshold energy by a constant $-\delta/2$. The relative motion of incident atoms is in the transverse ground state $\phi_{n=0,m_z=0}(\rho)$, where $\rho=\sqrt{x^2+y^2}$, $n=0,1,2,\ldots$ is the transverse principle quantum number, and $m_z=n,n-2,n-4,\ldots,\xi_n$ is the quantum number for the angular momentum along the z direction. Here $\xi_n=0$ (1) when n is even (odd). Since the system is invariant under the rotation along the z direction, m_z is conserved and only the transverse states with $m_z=0$ are involved in this problem. We further assume that both the Zeeman energy δ and the relative kinetic energy ϵ of the two atoms in the channel $|g\downarrow;e\uparrow\rangle$ are much smaller than the energy gap $2\hbar\omega$ between the first transverse excited state and the transverse ground state, i.e.,

$$\epsilon,\delta \ll 2\hbar\omega. \tag{A2}$$

In this system the two-atom scattering wave function can be written as

$$|\Psi(\mathbf{r})\rangle=\Psi^{(\uparrow\downarrow)}(z,\rho)|g\uparrow;e\downarrow\rangle+\Psi^{(\downarrow\uparrow)}(z,\rho)|g\downarrow;e\uparrow\rangle, \tag{A3}$$

where the functions $\Psi^{(\uparrow\downarrow)}(z,\rho)$ and $\Psi^{(\downarrow\uparrow)}(z,\rho)$ are given by

$$\Psi^{(\uparrow\downarrow)}(z,\rho)=[\alpha e^{ik^{(\uparrow\downarrow)}z}+f^{(\uparrow\downarrow)}e^{ik^{(\uparrow\downarrow)}|z|}]\phi_{n=0,m_z=0}(\rho)+\sum_{n=2,4,6,8,\ldots}B_n^{(\uparrow\downarrow)}e^{-\kappa_n^{(\uparrow\downarrow)}|z|}\phi_{n,m_z=0}(\rho), \tag{A4}$$

$$\Psi^{(\downarrow\uparrow)}(z,\rho)=[\beta e^{ik^{(\downarrow\uparrow)}z}+f^{(\downarrow\uparrow)}e^{ik^{(\downarrow\uparrow)}|z|}]\phi_{n=0,m_z=0}(\rho)+\sum_{n=2,4,6,8,\ldots}B_n^{(\downarrow\uparrow)}e^{-\kappa_n^{(\downarrow\uparrow)}|z|}\phi_{n,m_z=0}(\rho). \tag{A5}$$

Here we consider the general case where ϵ could be either larger or smaller than δ. When $\epsilon<\delta$, the incident atoms are in the state $|g\downarrow;e\uparrow\rangle$, which means $(\alpha,\beta)=(0,1)$. When $\epsilon>\delta$, the incident atoms are in the state $|g\uparrow;e\downarrow\rangle$ or $|g\downarrow;e\uparrow\rangle$, which means either $(\alpha,\beta)=(1,0)$ or $(\alpha,\beta)=(0,1)$ for the system. In Eqs. (A4) and (A5) the function $\phi_{n,m_z}(\rho)$ is the eigenwave function of the transverse Hamiltonian (i.e., the Hamiltonian of a two-dimensional harmonic oscillator in the $x-y$ plane with frequency ω) with quantum numbers (n,m_z), which satisfies $\phi_{n,m_z=0}(\rho=0)=1/\sqrt{\pi}a_\perp$, with $a_\perp=\sqrt{\hbar/\mu\omega}$ being the characteristic length of the transverse confinement. The parameters $k^{(\uparrow\downarrow)}$, $k^{(\downarrow\uparrow)}$, $\kappa_n^{(\uparrow\downarrow)}$, and $\kappa_n^{(\downarrow\uparrow)}$ are given by

$$k^{(\uparrow\downarrow)}=\sqrt{\frac{2\mu(\epsilon-\delta)}{\hbar^2}},\quad \kappa_n^{(\uparrow\downarrow)}=\sqrt{\frac{2\mu(2n\hbar\omega+\delta-\epsilon)}{\hbar^2}},$$
$$k^{(\downarrow\uparrow)}=\sqrt{\frac{2\mu\epsilon}{\hbar^2}},\quad \kappa_n^{(\downarrow\uparrow)}=\sqrt{\frac{2\mu(2n\hbar\omega-\epsilon)}{\hbar^2}}, \tag{A6}$$

while the scattering amplitudes $f^{(\uparrow\downarrow)}$ and $f^{(\downarrow\uparrow)}$ and the coefficients $B_n^{(\uparrow\downarrow)}$ and $B_n^{(\downarrow\uparrow)}$ can be obtained from the Schrödinger equation

$$\hat{H}_c|\Psi(\mathbf{r})\rangle=(\epsilon+\hbar\omega)|\Psi(\mathbf{r})\rangle, \tag{A7}$$

where the term $\hbar\omega$ on the right-hand side of Eq. (A7) is contributed by the zero-point energy of the transverse ground state.

Substituting Eqs. (A4) and (A5) into Eq. (A7) and performing the operation

$$\frac{1}{\sqrt{2\pi}}\lim_{\varepsilon\to0}\int_{-\varepsilon}^{+\varepsilon}dz\int_0^\infty\rho\,d\rho\,\phi^*_{n,m_z=0}(\rho)$$

on both sides of Eq. (A7), we can obtain the relations

$$f^{(\uparrow\downarrow)}=-i\frac{2\sqrt{\pi}}{k^{(\uparrow\downarrow)}a_\perp}(a_{s0}\eta^{(\uparrow\downarrow)}+a_{s1}\eta^{(\downarrow\uparrow)}), \tag{A8}$$

$$B_n^{(\uparrow\downarrow)}=-\frac{2\sqrt{\pi}}{\kappa_n^{(\uparrow\downarrow)}a_\perp}(a_{s0}\eta^{(\uparrow\downarrow)}+a_{s1}\eta^{(\downarrow\uparrow)}), \tag{A9}$$

$$f^{(\downarrow\uparrow)}=-i\frac{2\sqrt{\pi}}{k^{(\downarrow\uparrow)}a_\perp}(a_{s0}\eta^{(\downarrow\uparrow)}+a_{s1}\eta^{(\uparrow\downarrow)}), \tag{A10}$$

$$B_n^{(\downarrow\uparrow)}=-\frac{2\sqrt{\pi}}{\kappa_n^{(\downarrow\uparrow)}a_\perp}(a_{s0}\eta^{(\downarrow\uparrow)}+a_{s1}\eta^{(\uparrow\downarrow)}), \tag{A11}$$

where

$$\eta^{(\uparrow\downarrow)}=\frac{\partial}{\partial z}[z\Psi^{(\uparrow\downarrow)}(z,\rho=0)]\Big|_{z\to0^+}, \tag{A12}$$

$$\eta^{(\downarrow\uparrow)}=\frac{\partial}{\partial z}[z\Psi^{(\downarrow\uparrow)}(z,\rho=0)]\Big|_{z\to0^+}. \tag{A13}$$

Furthermore, substituting Eqs. (A9) and (A11) into Eqs. (A4) and (A5) and using the fact that $\phi_{n,m_z=0}(\rho=0)=1/\sqrt{\pi}a_\perp$, we obtain

$$\Psi^{(\uparrow\downarrow)}(z,\rho=0)=\frac{\alpha e^{ik^{(\uparrow\downarrow)}z}}{\sqrt{\pi}a_\perp}-[a_{s0}\eta^{(\uparrow\downarrow)}+a_{s1}\eta^{(\downarrow\uparrow)}]\times\left\{i\frac{2e^{ik^{(\uparrow\downarrow)}|z|}}{\hbar k^{(\uparrow\downarrow)}a_\perp^2}+\frac{\Lambda\left[\frac{2|z|}{a_\perp},-\left(\frac{k^{(\uparrow\downarrow)}}{2}a_\perp\right)^2\right]}{\hbar a_\perp}\right\}, \tag{A14}$$

$$\Psi^{(\downarrow\uparrow)}(z,\rho=0)=\frac{\beta e^{ik^{(\downarrow\uparrow)}z}}{\sqrt{\pi}a_\perp}-[a_{s0}\eta^{(\downarrow\uparrow)}+a_{s1}\eta^{(\uparrow\downarrow)}]\times\left\{i\frac{2e^{ik^{(\downarrow\uparrow)}|z|}}{\hbar k^{(\downarrow\uparrow)}a_\perp^2}+\frac{\Lambda\left[\frac{2|z|}{a_\perp},-\left(\frac{k^{(\downarrow\uparrow)}}{2}a_\perp\right)^2\right]}{\hbar a_\perp}\right\}, \tag{A15}$$

where the function $\Lambda[\xi,\nu]$ is defined as $\Lambda[\xi,\nu]=\sum_{s'=1}^\infty e^{-\sqrt{s'+\nu}\xi}/\sqrt{s'+\nu}$. As shown in Ref. [18], this function can be expanded as

$$\Lambda[\xi,\nu]=\frac{2}{\xi}+\zeta\left[\frac{1}{2},1+\nu\right]+O(\xi), \tag{A16}$$

with $\zeta(s,a)$ being the Hurwitz zeta function. Substituting Eqs. (A14) and (A15) into Eqs. (A12) and (A13) and using Eq. (A16), we can obtain the factors $\eta^{(\downarrow\uparrow)}$ and $\eta^{(\uparrow\downarrow)}$. Further using these results and Eqs. (A8)–(A11), we can finally obtain the expressions of the scattering amplitudes $f^{(\uparrow\downarrow)}$ and $f^{(\downarrow\uparrow)}$:

$$\begin{pmatrix}f^{(\uparrow\downarrow)}\\ f^{(\downarrow\uparrow)}\end{pmatrix}=\frac{-1}{I+iAP+i\sum_{s=1}^\infty\left(\frac{\epsilon}{2\hbar\omega}\right)^sA'_sP}\begin{pmatrix}\alpha\\ \beta\end{pmatrix}, \tag{A17}$$

where I, A, P, and A'_s are ϵ-independent 2×2 matrices expressed as

$$I=\begin{pmatrix}1&0\\0&1\end{pmatrix},\quad P=\begin{pmatrix}k^{(\uparrow\downarrow)}&0\\0&k^{(\downarrow\uparrow)}\end{pmatrix}, \tag{A18}$$

and

$$A = -\frac{a_\perp^2}{2}\left[\begin{pmatrix} a_{s0} & a_{s1} \\ a_{s1} & a_{s0}\end{pmatrix}^{-1} + \begin{pmatrix} \frac{\zeta[\frac{1}{2},1+\frac{\delta}{2\hbar\omega}]}{a_\perp} & 0 \\ 0 & \frac{\zeta[\frac{1}{2},1]}{a_\perp}\end{pmatrix}\right]. \tag{A19}$$

The expressions of A'_s can be obtained by the straightforward calculation we introduced above and are not needed in the following discussion. In Eq. (A17), $\frac{1}{[\cdots]}$ means the inverse matrix of $[\cdots]$.

On the other hand, according to Eqs. (A4) and (A5), in the long-range limit $|z| \to \infty$ (i.e., $|z| \gg a_\perp$) the asymptotic wave function of the two-atom relative motion reads

$$|\Psi(\mathbf{r})\rangle \xrightarrow{|z|\to\infty} [(\alpha e^{ik^{(\uparrow\downarrow)}z} + f^{(\uparrow\downarrow)}e^{ik^{(\uparrow\downarrow)}|z|})|g\uparrow;e\downarrow\rangle + (\beta e^{ik^{(\downarrow\uparrow)}z} + f^{(\downarrow\uparrow)}e^{ik^{(\downarrow\uparrow)}|z|})|g\downarrow;e\uparrow\rangle]\phi_{0,0}(\rho). \tag{A20}$$

Therefore, the long-range behavior of the two-atom relative wave function is completely determined by Eq. (A17).

Now let us consider a pure one-dimensional system with the Hamiltonian $\hat{H}_{1D}$ defined in Eq. (9). Similar to the above, in the bases $\{|g\uparrow;e\downarrow\rangle, |g\downarrow;e\uparrow\rangle\}$, this Hamiltonian can be rewritten as

$$\hat{H}_{1D} = \left(-\frac{\hbar^2}{2\mu}\frac{d^2}{dz^2}\right)(\mathcal{P}_{\uparrow\downarrow} + \mathcal{P}_{\downarrow\uparrow}) + \delta\mathcal{P}_{\uparrow\downarrow} + \left[\frac{g_+ + g_- + 2g_c}{2}\mathcal{P}_{\uparrow\downarrow} + \frac{g_+ + g_- - 2g_c}{2}\mathcal{P}_{\downarrow\uparrow} + \frac{g_- - g_+}{2}(\mathcal{S}_{ex} + \mathcal{S}_{ex}^\dagger)\right]\delta(z). \tag{A21}$$

With straightforward calculation, it is easy to find that the one-dimensional scattering wave function in this system is given by

$$|\Psi_{1D}(z)\rangle = (\alpha e^{ik^{(\uparrow\downarrow)}z} + f_{1D}^{(\uparrow\downarrow)}e^{ik^{(\uparrow\downarrow)}|z|})|g\uparrow;e\downarrow\rangle + (\beta e^{ik^{(\downarrow\uparrow)}z} + f_{1D}^{(\downarrow\uparrow)}e^{ik^{(\downarrow\uparrow)}|z|})|g\downarrow;e\uparrow\rangle, \tag{A22}$$

with α, β, $k^{(\uparrow\downarrow)}$, and $k^{(\downarrow\uparrow)}$ defined the same as above, and the one-dimensional scattering amplitudes $f_{1D}^{(\uparrow\downarrow)}$ and $f_{1D}^{(\downarrow\uparrow)}$ are given by

$$\begin{pmatrix} f_{1D}^{(\uparrow\downarrow)} \\ f_{1D}^{(\downarrow\uparrow)}\end{pmatrix} = -\frac{1}{I + iA_{1D}P}\begin{pmatrix}\alpha \\ \beta\end{pmatrix}, \tag{A23}$$

where P is defined in Eq. (A18) and

$$A_{1D} = -\frac{2\hbar^2}{\mu}\begin{pmatrix} g_+ + g_- + 2g_c & g_- - g_+ \\ g_- - g_+ & g_+ + g_- - 2g_c\end{pmatrix}^{-1} \tag{A24}$$

is the one-dimensional scattering length matrix.

By comparing Eqs. (A17) and (A19) with Eqs. (A23) and (A24), we find that in the systems where ϵ is much smaller than $\hbar\omega$ so that the high-order terms $i\sum_{s=1}^{\infty}(\frac{\epsilon}{2\hbar\omega})^s A'_s P$ can be neglected in Eq. (A17), when the one-dimensional parameters

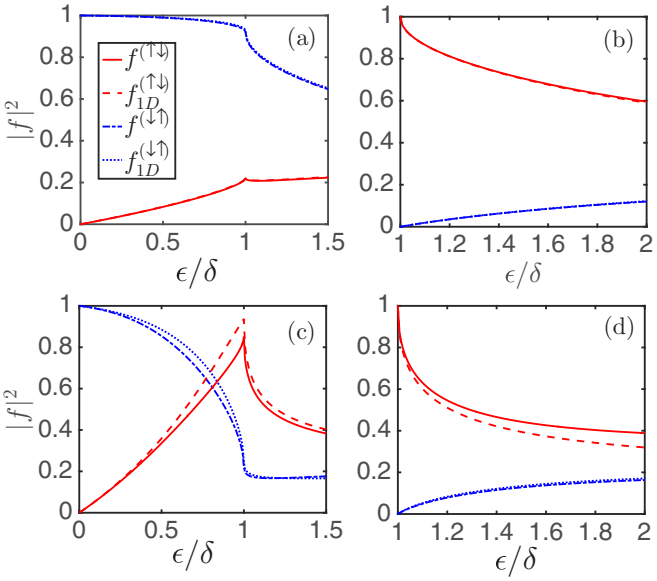

FIG. 6. Scattering amplitude as a function of incident energy (a) and (c) $\epsilon \gtrless 0$, where incident atoms are in state $|g\downarrow;e\uparrow\rangle(\alpha = 0, \beta = 1)$, with α and β defined in Eqs. (A4) and (A5), respectively, and (b) and (d) $\epsilon \gtrless \delta$, where incident atoms are in state $|g\uparrow;e\downarrow\rangle(\alpha = 1, \beta = 0)$. As shown in (a) and (b), if $\delta \approx 0.1\hbar\omega$, the scattering amplitude given by the 1D model almost coincides with that given by the complete calculation, while if $\delta \approx 0.4\hbar\omega$, the difference in the scattering amplitude appears, as shown in (c) and (d).

$g_\pm$ and g_c satisfy

$$\begin{pmatrix} a_{s0} & a_{s1} \\ a_{s1} & a_{s0}\end{pmatrix}^{-1} + \frac{1}{a_\perp}\begin{bmatrix}\zeta\left(\frac{1}{2},1+\frac{\delta}{2\hbar\omega}\right) & 0 \\ 0 & \zeta\left(\frac{1}{2},1\right)\end{bmatrix} = \frac{4\hbar}{\mu a_\perp^2}\begin{pmatrix} g_+ + g_- + 2g_c & g_- - g_+ \\ g_- - g_+ & g_+ + g_- - 2g_c\end{pmatrix}^{-1}, \tag{A25}$$

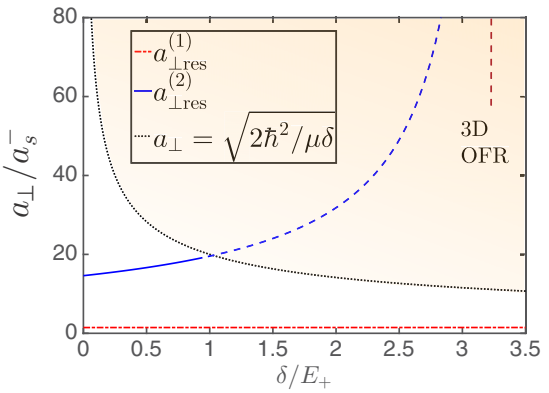

FIG. 7. Red and blue solid lines denote the positions $a_{\perp res}^{(1)}$ and $a_{\perp res}^{(2)}$ of the first and second CIR, respectively. The blue dashed line shows that if one extends the calculation to the limit of low trapping frequency, the position of the second CIR approaches the position of the orbital Feshbach resonance (OFR) in the 3D system [32], which is shown by the red dashed line. The black dotted line shows the condition $a_\perp = \sqrt{2\hbar^2/\mu\delta}$. Our effective 1D model is applicable only in the region with $a_\perp < \sqrt{2\hbar^2/\mu\delta}$, i.e., the region below the dotted line.

we have the relation $A \approx A_{1D}$, which gives

$$f_{1D}^{(\uparrow\downarrow)} \approx f^{(\uparrow\downarrow)}, \quad f_{1D}^{(\downarrow\uparrow)} \approx f^{(\downarrow\uparrow)} \tag{A26}$$

and

$$|\Psi(\mathbf{r})\rangle \xrightarrow{|z|\to\infty} \phi_{n=0,m_z=0}(\rho)|\Psi_{1D}(z)\rangle. \tag{A27}$$

Therefore, the Hamiltonian $\hat{H}_{1D}$ in Eq. (9) with the parameters $g_\pm$ and g_c given by Eq. (A25) is the correct one-dimensional model for these systems and the values of g_+, g_-, and g_c at finite magnetic field are plotted in Fig. 2(b). In Fig. 6 we plot $f^{(\uparrow\downarrow)}$ and $f^{(\downarrow\uparrow)}$ given by the complete calculation [i.e., Eq. (A17)] and $f_{1D}^{(\uparrow\downarrow)}$ and $f_{1D}^{(\downarrow\uparrow)}$ from the one-dimensional model [i.e., Eq. (A23)]. It is shown that as long as δ is small enough, the scattering amplitude given by the one-dimensional model almost coincides with that given by the complete calculation, no matter where the incident channel is located, as shown in Figs. 6(a) and 6(b). However, when δ is comparable to $\hbar\omega$, the difference between these scattering amplitudes in the high-energy regime begins appears, as shown in Figs. 6(c) and 6(d).

In Fig. 7 we show the characteristic length $a_{res}^{(1,2)}$ for the first and second CIRs as a function of the Zeeman energy δ. The position of the first CIR is insensitive to the Zeeman field, while that of the second CIR is quite sensitive to the Zeeman field. It should be noted that since our calculation is based on the condition (A2), the effective one-dimensional model is applicable only in the parameter region $\delta < 2\hbar\omega$ or $a_\perp < \sqrt{2\hbar^2/\mu\delta}$, i.e., the light region below the dotted line in Fig. 7.

[1] N. Hinkley, J. A. Sherman, N. B. Phillips, M. Schioppo, N. D. Lemke, K. Beloy, M. Pizzocaro, C. W. Oates, and A. D. Ludlow, Science **341**, 1215 (2013); B. J. Bloom, T. L. Nicholson, J. R. Williams, S. L. Campbell, M. Bishof, X. Zhang, W. Zhang, S. L. Bromley, and J. Ye, Nature (London) **506**, 71 (2014).

[2] S. Taie, R. Yamazaki, S. Sugawa, and Y. Takahashi, Nat. Phys. **8**, 825 (2012).

[3] G. Pagano, M. Mancini, G. Cappellini, P. Lombardi, F. Schäfer, H. Hu, X. J. Liu, J. Catani, C. Sias, M. Inguscio, and L. Fallani, Nat. Phys. **10**, 198 (2014).

[4] X. Zhang, M. Bishof, S. L. Bromley, C. V. Kraus, M. S. Safronova, P. Zoller, A. M. Rey, and J. Ye, Science **345**, 1467 (2014).

[5] F. Scazza, C. Hofrichter, M. Höfer, P. C. De Groot, I. Bloch, and S. Fölling, Nat. Phys. **10**, 779 (2014); **11**, 514 (2015).

[6] G. Cappellini, M. Mancini, G. Pagano, P. Lombardi, L. Livi, M. Siciliani de Cumis, P. Cancio, M. Pizzocaro, D. Calonico, F. Levi, C. Sias, J. Catani, M. Inguscio, and L. Fallani, Phys. Rev. Lett. **113**, 120402 (2014); **114**, 239903(E) (2015).

[7] M. A. Cazalilla and A. M. Rey, Rep. Prog. Phys. **77**, 124401 (2014).

[8] A. V. Gorshkov, M. Hermele, V. Gurarie, C. Xu, P. S. Julenne, J. Ye, P. Zoller, E. Demler, M. D. Lukin, and A. M. Rey, Nat. Phys. **6**, 289 (2010).

[9] G. M. Falco, R. A. Duine, and H. T. C. Stoof, Phys. Rev. Lett. **92**, 140402 (2004).

[10] L.-M. Duan, Europhys. Lett. **67**, 721 (2004).

[11] A. Recati, P. O. Fedichev, W. Zwerger, J. von Delft, and P. Zoller, Phys. Rev. Lett. **94**, 040404 (2005).

[12] B. Paredes, C. Tejedor, and J. I. Cirac, Phys. Rev. A **71**, 063608 (2005).

[13] P. P. Orth, I. Stanic, and K. Le Hur, Phys. Rev. A **77**, 051601 (2008).

[14] Y. Nishida, Phys. Rev. Lett. **111**, 135301 (2013); Phys. Rev. A **93**, 011606 (2016).

[15] J. Bauer, C. Salomon, and E. Demler, Phys. Rev. Lett. **111**, 215304 (2013).

[16] I. Kuzmenko, T. Kuzmenko, Y. Avishai, and K. Kikoin, Phys. Rev. B **91**, 165131 (2015).

[17] L. Isaev and A. M. Rey, Phys. Rev. Lett. **115**, 165302 (2015).

[18] M. Olshanii, Phys. Rev. Lett. **81**, 938 (1998).

[19] T. Bergeman, M. G. Moore, and M. Olshanii, Phys. Rev. Lett. **91**, 163201 (2003).

[20] E. Haller, M. J. Mark, R. Hart, J. G. Danzl, L. Reichsollner, V. Melezhik, P. Schmelcher, and H.-C. Nägerl, Phys. Rev. Lett. **104**, 153203 (2010).

[21] A. C. Hewson, *The Kondo Problem to Heavy Fermions* (Cambridge University Press, Cambridge, 1993).

[22] Z. W. Barber, J. E. Stalnaker, N. D. Lemke, N. Poli, C. W. Oates, T. M. Fortier, S. A. Diddams, L. Hollberg, C. W. Hoyt, A. V. Taichenachev, and V. I. Yudin, Phys. Rev. Lett. **100**, 103002 (2008).

[23] M. Höfer, L. Riegger, F. Scazza, C. Hofrichter, D. R. Fernandes, M. M. Parish, J. Levinsen, I. Bloch, and S. Fölling, Phys. Rev. Lett. **115**, 265302 (2015).

[24] G. Pagano, M. Mancini, G. Cappellini, L. Livi, C. Sias, J. Catani, M. Inguscio, and L. Fallani, Phys. Rev. Lett. **115**, 265301 (2015)

[25] M. M. Boyd, T. Zelevinsky, A. D. Ludlow, S. Blatt, T. Zanon-Willette, S. M. Foreman, and J. Ye, Phys. Rev. A **76**, 022510 (2007).

[26] X. Cui, Phys. Rev. A **90**, 022705 (2014).

[27] D. H. Lee and J. Toner, Phys. Rev. Lett. **69**, 3378 (1992).

[28] A. Furusaki and N. Nagaosa, Phys. Rev. Lett. **72**, 892 (1994).

[29] D. P. Zhang, W. Chen, and H. Zhai, arXiv:1510.08303.

[30] P. W. Anderson, J. Phys. C **3**, 2436 (1970).

[31] C. Sanner, E. J. Su, A. Keshet, W. Huang, J. Gillen, R. Gommers, and W. Ketterle, Phys. Rev. Lett. **106**, 010402 (2011).

[32] R. Zhang, Y. Cheng, H. Zhai, and P. Zhang, Phys. Rev. Lett. **115**, 135301 (2015).